Available online at www.sciencedirect.com
ScienceDirect
Polymer 48 (2007) 5059–5068
polymer
www.elsevier.com/locate/polymer

Syntheses and characterizations of the multiple morphologies formed by the self-assembly of the semicrystalline P4VP-*b*-PCL diblock copolymers

Shih-Chi Chan [a], Shiao-Wei Kuo [b,**], Chu-Hua Lu [a], Hsin-Fang Lee [a], Feng-Chih Chang [a,*]

[a] *Institute of Applied Chemistry, National Chiao Tung University, Hsin Chu, Taiwan*
[b] *Department of Materials and Optoelectronic Engineering, National Sun Yat-Sen University, Kaohsiung, Taiwan*

Received 8 February 2007; received in revised form 12 June 2007; accepted 22 June 2007
Available online 28 June 2007

Abstract

A series of semicrystalline diblock copolymers of poly(4-vinylpyridine-*b*-ε-caprolactone) (P4VP-*b*-PCL) have been synthesized by the living ROP of CL followed by the TEMPO polymerization of 4-VP. Depending on the relative block length and different solvent compositions, these copolymers self-assemble into different supramolecular structures in toluene/dichloromethane (DCM) solution, including spherical micelles, bowl-shaped vesicles, multilayer vesicles, porous spheres, and large compound micelles. In methanol/DCM solution system, the crystalline PCL core disturbs the balance of free energy, thus results in a series of morphological changes including spherical micelles, worm-like rods, vesicles, coexisted vesicles and lamella, and finally platelet lamella.

Keywords: Block copolymer; TEMPO; Self-assembly

1. Introduction

Block copolymers have received considerable attention due to their ability to self-assemble in bulk or in solution forming a range of different morphologies and sizes [1–7]. In solution, they spontaneously self-assemble into well-defined micelles or aggregates in the presence of a selective solvent for one of the blocks [8–19]. In the pioneer work reported by Eisenberg and coworkers, multiple morphologies of micelles made from linear block copolymers, such as spheres, rods, vesicles and large compound micelles (LCMs), have been observed [19–21]. Many other scientists have designed and prepared various new materials with special architecture in order to obtain novel self-assembled objects with particular morphologies [21–26]. The compositions of block copolymers can be tuned to affect the formation of micelles or aggregates of shapes other than spheres in block-selective solvents, as demonstrated by the seminal work of Eisenberg [19,21] and others [7,22]. Depending on the composition of the block copolymers, two types of micelles can be distinguished: star and crew-cut micelles [27]. The star micelles have relatively large shells consisting of the long soluble block and the relatively small core consisting of the short insoluble block. Aggregates of another kind, namely crew-cuts, have cores whose dimension is relatively larger than that of shells. Generally, star micelles can be prepared directly by dissolving a highly asymmetric block copolymer, e.g., polystyrene-*b*-poly(acrylic acid) (PS-*b*-PAA), in a solvent selective for the long block or by adding water into polymer solution in a common solvent of *N*,*N*-dimethylformamide (DMF), while crew-cut micelles are usually prepared by the water addition method in most cases [19].

Block copolymer micelles, which can be either thermodynamically or kinetically stable under a given set of conditions or aggregates, have many potential applications in various fields, such as cosmetics, drug delivery, electronics, pollution control, advanced materials formation, separation, among others [28–31]. It has been known that the equilibrium

* Corresponding author. Tel.: +886 3 5131512; fax: +886 3 5719507.
** Corresponding author. Tel.: +886 7 5252000x4709.
E-mail addresses: kuosw@mail.nsysu.edu.tw (S.-W. Kuo), changfc@mail.nctu.edu.tw (F.-C. Chang).

0032-3861/$ - see front matter © 2007 Elsevier Ltd. All rights reserved.
doi:10.1016/j.polymer.2007.06.053

aggregate morphologies can be controlled by altering the influence exerted by a given parameter on the interplay of three major components of the free energy of the aggregates [32,33]. These components include the stretching of core-forming blocks, intercorona interactions, and the interfacial free energy between the solvent and the micellar core. Changing any of these factors disturbs the balance between the forces governing the aggregates, leading to the transformation of one morphology into another. There are many factors that affect the above three components, and by varying one or more of these, the morphologies can then, in principle, be fine-tuned. Examples of such factors that have been studied previously include relative block lengths of the copolymer, initial copolymer concentration in solutions, common solvent used, precipitant, temperature, type and amount of the adding ions (salt, acid, or base), etc. [34].

A series of semicrystalline P4VP-*b*-PCL block copolymers were prepared herein via a new synthetic procedure by anionic ring-opening polymerization of ε-caprolactone followed by living nitroxide-mediated free radical polymerization (NMP) of 4-vinylpyridine with a bifunctional initiator.

The crystalline polyester of ε-caprolactone is an important biodegradable and biocompatible material. Aluminum alkoxides are used to synthesize the designed polymers based on PCL. Ring-opening polymerization mediated by aluminum alkoxide has proved to precede a living polymerization and leads to the controlled synthesis of oligomers and block copolymers with functional groups at the chain ends [35]. These functional groups, associated with the active alkoxy moiety of the aluminum alkoxide, can selectively attach to one chain end of PCL. Yoshida and Sugita have reported the synthesis of poly(THF-*block*-styrene) with a bifunctional initiator 4-oxo-TEMPO [36]. The development of this quantitative synthesis of the block copolymer has been obtained by many investigators, concerning the styrene polymerization using 2,2,6,6-tetramethylpiperidinyloxy (TEMPO) [37,38]. Herein, we use 4-hydroxy-TEMPO as initiator to synthesize PCL with TEMPO as an end-functional group, followed by copolymerization of 4-vinylpyridine through the living radical polymerization using the TEMPO–PCL as a counter radical.

TEMPO has been found to be able to serve as a ''counter radical'' in living radical polymerization to give polymers with narrow polydispersities [39]. Nitroxide radicals have proved to be able to protect the active center of each growing chain by capping it, occasionally releasing it to permit the insertion of a monomer unit [40]. The genesis of this field can be traced back to the pioneering work of Rizzardo [41], the stimulus for the current interest is the seminal report of Georges et al. [42] that narrow polydispersity polystyrene (<1.3) can be prepared using a mixture of benzoyl peroxide (BPO) and 2,2,6,6-tetramethylpiperidinyloxy (TEMPO) as an initiating system. Although nitroxide-mediated radical polymerization (NMRP) was originally devoted to study the styrene monomer, the preparations of other well-defined polymers from reactive monomers have also been demonstrated in a number of cases [43]. However, there were still few reports using 4-vinylpyridine as a potential monomer for controlled free radical polymerization since the first works of Bohrisch et al. in 1997 [44]. Considering that the nitrogen atom of the pyridine ring of P4VP can trap metal ions, the metal free NMRP procedure for polymerization of 4-vinylpyridine can be easily purified comparing to other living radical polymerization methods.

In this report, two different functional groups on a single initiator are used to initiate living ring-opening and ''living'' free radical polymerizations. We also report detailed experimental results concerning various morphologies of the micelle aggregates for the diblock copolymer P4VP-*b*-PCL in toluene/DCM and methanol/DCM solvents.

2. Experimental

2.1. Materials

All chemicals were purchased form Aldrich. ε-Caprolactone and 4-vinylpyridine were purified by distillation before use. 4-Hydroxy-TEMPO (4-hydroxy 2,2,6,6-tetramethylpiperidinyloxy) and triethylaluminum (25% in toluene) were used without further purification. Benzoyl peroxide was precipitated from chloroform and then recrystallized in methanol at 0 °C. Toluene and THF were reflux over *n*-BuLi for several hours and then distilled just before use.

2.2. Synthesis of TEMPO-terminated PCL

All PCL samples were synthesized according to prior literature [36]. 4-Hydroxy-TEMPO (0.54 g, 3.12 mol) was dissolved in 10 mL dried THF at room temperature under a nitrogen atmosphere and triethylaluminum (25 wt% toluene solution, 0.7 mL, 1.04 mmol) was added. The mixture was stirred at room temperature for 1 h and kept at 40 °C for 2 h under a nitrogen atmosphere, and then dried *in vacuo* for 1 h at 40 °C to remove the THF. Toluene (30 mL) was then added to the resultant mixture and kept at 40 °C for 1 h, and then cooled to room temperature. ε-CL (6.0 mL, 54.2 mmol) was added to the mixture and stirred. The solution was kept for 8 h at room temperature under nitrogen, and then 1 mL of distilled water was added to terminate the polymerization. The solution was washed three times with the 0.01 N aqueous solution of EDTA, and another three times with water. The toluene layer was dried over anhydrous magnesium sulfate and then evaporated to remove toluene. The product was purified by repeated precipitations from toluene into hexane, and dried *in vacuo* for several hours to yield 5.5 g of PCL (yield: 91%).

2.3. Synthesis of P4VP-b-PCL

4-Vinylpyridine (2.25 g, 21.46 mmol), BPO (14 mg, 0.06 mmol), and TEMPO-terminated PCL (0.5 g, containing 0.075 mmol of TEMPO moiety) were placed in a Schlenk flask equipped with a reflux condenser and a magnetic stirrer. After degassing procedure, the polymerization was carried out for 3.5 h at 95 °C, and then continued for another 48 h at 125 °C. The polymerization was terminated by cooling with

liquid nitrogen. The product was then dissolved in 10 mL of dichloromethane, purified by repeated precipitations from dichloromethane into hexane, and finally dried *in vacuo* for several hours to yield 2 g of the block copolymer (yield: 73%).

2.4. Preparation of micelle solutions

The diblock copolymer was first dissolved in dichloromethane (DCM), a common solvent for both poly(4-vinylpyridine) and poly(ε-caprolactone) blocks. The second solvent was added slowly to the stirred polymer solution via a syringe pump at a constant rate. Typical addition rate was 1–5 mL/h. In order to estimate the ideal solvent composition for the formation of micelles, addition of solvent was continued until the solution turned turbid during the first trial. In subsequent experiments, addition was stopped before the appearance of turbidity. Stirring of solution was continued for 2 days before further characterizations.

2.5. Characterizations

Differential scanning calorimetry (DSC) of the material was performed under a continuous nitrogen flow (60 mL/min) using a TA Instrument DSC 2910. Each sample was first heated to 200 °C and maintained isothermally for 5 min, then was quickly quenched to −110 °C. Data were gathered on the second heating cycle at a scan rate of 20 °C/min over a temperature range from −110 to 200 °C. The glass transition temperature was taken as the midpoint of the heat capacity transition between the upper and lower points of the deviation from the extrapolated glass and liquid lines. Fourier transform IR spectra were obtained using a Nicolet Avatar 320 FTIR Spectrometer, 32 scans were collected with a spectral resolution of 1 cm^{-1}. The conventional KBr disk method was employed. A THF solution containing the sample was cast onto a KBr disk and dried under conditions similar to those used in the bulk preparation. The holder was placed in the sample chamber and the spectrum was recorded under an N_2 purge to maintain the film's dryness. The weight-average (M_w), number-average (M_n) molecular weights and the polydispersity index (M_w/M_n) were measured using a Waters 410 gel permeation chromatography (GPC) system equipped with RI and UV detectors and a Styragel column (300 × 7.8 mm). The system was calibrated using polystyrene standards, the eluent was DMF, and the flow rate was 1.0 mL/min. ^{1}H NMR spectroscopic analyses were performed using a Varian Uniytinova-500 NMR Spectrometers at 500 MHz. All spectra were recorded using $CDCl_3$ as the solvent and TMS as the external standard. The ^{13}C CP/MAS NMR spectra were recorded at room temperature using a Bruker DSX-400WB NMR Spectrometer with a sample spinning rate of 8.0 kHz. The spectra were acquired using a 3.9-μs proton 90° pulse, a 1-ms contact time, and a 3-s repetition time. Ultraviolet (UV) spectra were obtained with a Beckman DU-68 Spectrophotometer. TEM were performed on a Hitachi H-7500 Transmission Electron Microscope at an acceleration voltage of 100 kV. A drop of the very dilute solution was placed onto a carbon-coated TEM copper grid. After 3 min, excess solution was blotted away using a strip of filter paper. The samples were allowed to dry in atmosphere at room temperature and then stained by osmium tetraoxide.

3. Results and discussion

3.1. Synthesis of poly(ε-caprolactone) with TEMPO at the chain end

Scheme 1 shows the basic outline for the strategy to prepare a series of P4VP-*b*-PCL copolymers. The bifunctional ligand aminoxy initiators 4-hydroxy-TEMPO contains a hydroxy group which is used as the initiating center for the living ring-opening polymerization of the cyclic lactone in the first step. The aminoxy group is an efficient initiator for preparation subsequent the nitroxide-mediated "living" free radical polymerization of the vinyl monomer in the second step. In the first step, living ROP of CL was achieved using 4-hydroxy-TEMPO and triethylaluminum as the initiation systems under strictly anhydrous condition, producing TEMPO–PCL products with narrow molecular weight distribution and predictable molecular weight. The TEMPO associated aluminum alkoxide

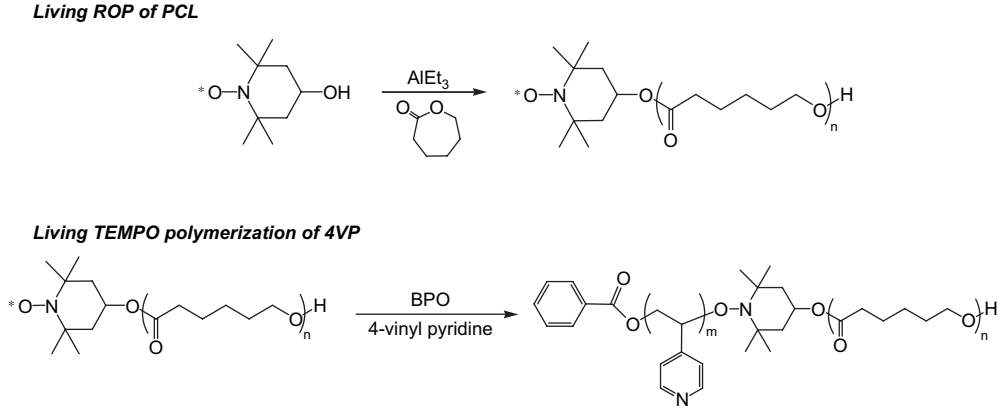

Scheme 1. Procedure of polymerization of the block copolymer.

was prepared by reacting triethylaluminum with 4-hydroxy-TEMPO. Since the TEMPO cannot tolerate coexistence with a strong base of alkylaluminum and tends to convert into the corresponding alkoxyamines, an aluminum tri(4-oxy-TEMPO) was prepared by reacting triethylaluminum with three equimolar amount of 4-hydroxy-TEMPO and used as an initiator for the CL polymerization according to the literature [36]. The reaction was carried out in THF at room temperature for 1 h and continued at 40 °C for another 2 h. The resulted aluminum tri(4-oxy-TEMPO) was used to initiate the polymerization with 4-VP monomer via a ''coordination–insertion'' mechanism [45]. The polymerization was performed in toluene at ambient temperature for 8 h, and the solution was red in color due to the presence of the TEMPO. After purification, a light red colored product was obtained. Typical molecular weight dispersity by GPC shows a unimodal curve. A typical GPC curve (**H2** in Table 1) is shown in Fig. 1a and all the results are summarized in Table 1, indicating that all polymers exhibit relatively narrow polydispersities, indicating that neither intra- nor intermolecular transesterification reaction occurred in the presence of aluminum alkoxide catalyst.

Fig. 2a shows the ^{1}H NMR spectrum of the resulting TEMPO–PCL polymer (**H2**). Besides the main characteristic peaks from PCL, peaks from the residual initiator moiety are hardly seen in the magnified area since the TEMPO moiety is not reduced into the corresponding hydroxylamine by any reagent. The molecular weights calculated from ^{1}H NMR analysis are lower than those obtained by GPC analysis based on polystyrene standards, as shown in Table 1. In order to confirm that TEMPO was indeed incorporated into PCL with single alkoxyamine chain end per macromolecule, UV spectral analysis was performed. Fig. 3 shows the UV spectrum of the resulting TEMPO–PCL (**H2**) where the polymer shows a characteristic absorption λ_{max} at 460 nm originating from the nitroxyl radical [36]. The absorbance intensity at 460 nm was calibrated with 4-OH-TEMPO. The content of the TEMPO attached to the polymer chain end is calculated by the absorbance at 460 nm and the molecular weight can also be calculated based on this value. The molecular weights thus determined are in a good agreement with those estimated by ^{1}H NMR (Table 1).

In addition, all TEMPO–PCLs exhibit the presence of terminal TEMPO attached to the PCL because they all manifest three sharp signals due to TEMPO in their electron spin resonance (ESR) spectra. Fig. 4 illustrates a typical ESR spectrum of the TEMPO–PCL (**H2**). All these g values and hyperfine coupling constants (AN) from these three sharp signals are almost identical to those of 4-OH-TEMPO (g: 2.00704, AN: 15.88 G). These results suggest that the stability of TEMPO attached to the PCL chain end is not affected by the PCL chain under these conditions, and therefore, these polymeric TEMPOs have the potential to serve as counter radicals in living radical polymerization in the same manner as monomeric TEMPO. Thus, the TEMPO functionalized PCL was elected to initiate the polymerization of vinyl monomers.

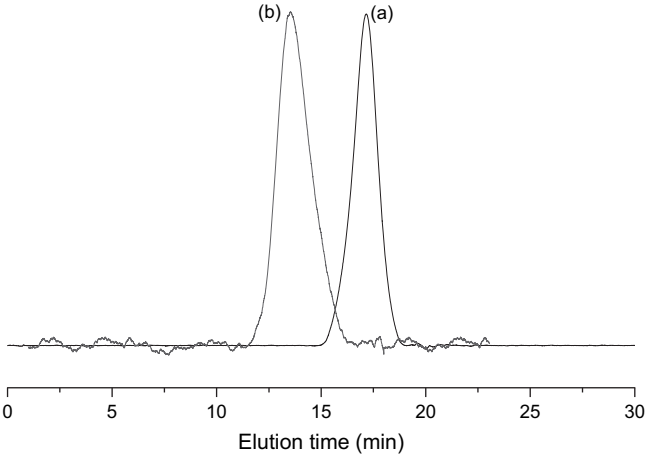

Fig. 1. GPC profiles of (a) tempo-terminated PCL prepolymer (Table 1, **H2**) and (b) the block copolymer (Table 2, **B2**).

3.2. ''Living'' free radical polymerization of 4-vinylpyridine in the presence of TEMPO-terminated PCL

The controlled radical polymerization of various monomers in the presence of *N*-oxyl radicals has been developed into a common way to produce polymers with well-defined architecture as well as controlled molecular weights with narrow polydispersities [38,39]. 4-Vinylpyridine is known to polymerize spontaneously at higher temperatures and is more reactive than styrene under the conditions of the free radical polymerization [46]. It has been found that the rate of polymerization is substantially faster with the TEMPO attached to a polymer than that with TEMPO of low molecular weight [36]. In this

Table 1
Summary of polymerization results of ROP of ε-caprolactone using 4-OH-TEMPO initiator and Et_3Al as initiation system

Entry	$[M]_0/[I]_0$	M_n[a] (NMR)	M_n[b] (GPC)	M_n[c] (UV)	Conv[d] (%)	M_w/M_n[e]	Content of TEMPO[f] (mmol/g)
H1	26	2680	4600	3000	77.3	1.33	0.33
H2	80	6000	15 700	5340	72.7	1.29	0.19
H3	200	10 400	26 300	9910	46.0	1.30	0.10
H4	300	22 800	47 400	21 300	65.1	1.37	0.05

[a] Estimated by ^{1}H NMR based on the relative intensity of the terminal hydroxymethylene and the methylene ($OC(O)CH_2$–: 2.3 ppm) in the PCL main chain.
[b] Determined by GPC using PS standards.
[c] Estimated by UV spectroscopy based on the content of TEMPO.
[d] Determined from ^{1}H NMR spectrum using the ratio of ester methylene peaks of poly(ε-caprolactone) (PCL) and ε-caprolactone.
[e] Polydispersity index: determined by GPC.
[f] Calculated by UV spectroscopy based on the absorbance at 460 nm.

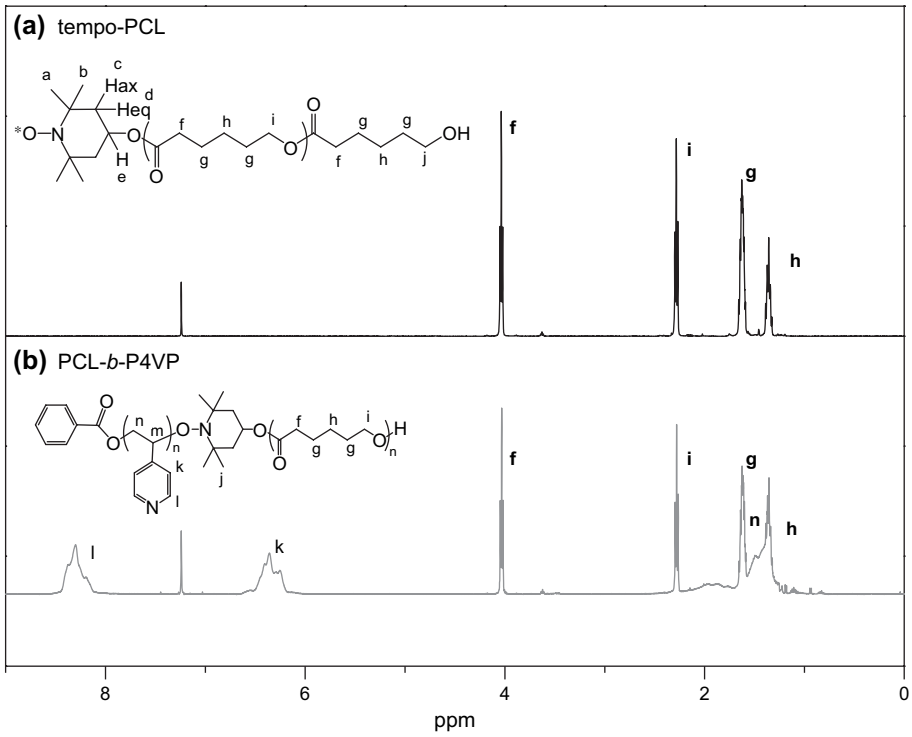

Fig. 2. ^{1}H NMR spectrum of (a) tempo-terminated PCL prepolymer (Table 1, **H2**) and (b) the block copolymer (Table 2, **B2**).

work, we use TEMPO-terminated PCL macroinitiator to enhance the polymerization rate of the 4-vinylpyridine monomer via nitroxide-mediated polymerization (NMP).

Scheme 1 depicts the polymerization of 4-vinylpyridine using benzoyl peroxide as an initiator and TEMPO as a capping agent. This approach is similar to the method reported by Georges et al. [42]. The polymerization was carried out in bulk at 130 °C after being held at 95 °C for 3.5 h. This two-step procedure of heating has the potential to give block copolymers with narrow polydispersities by separating the initiation from the propagation. The polymerization was stopped at low monomer conversion to avoid the gel effect. After purification, the resulted copolymers were confirmed by a number of different techniques. Fig. 2b shows typical ^{1}H NMR spectrum of the resulting P4VP-*b*-PCL copolymer (**B2** in Table 2). In addition to the signals due to CL, the broad signals at 6.2–6.4 and 8.2–8.4 ppm can be assigned to the protons of the pyridine rings of the 4-vinylpyridine. The signals of protons from TEMPO and aromatic ring of benzoyl are not clearly observed because of their low molar ratio in the block copolymer. FTIR spectra further confirm the result as shown in Fig. 5 displaying the spectrum of resulting block copolymer **B2**. Besides the characteristic peak at 1730 cm^{-1} of PCL, the appearance of the characteristic peak of pyridine

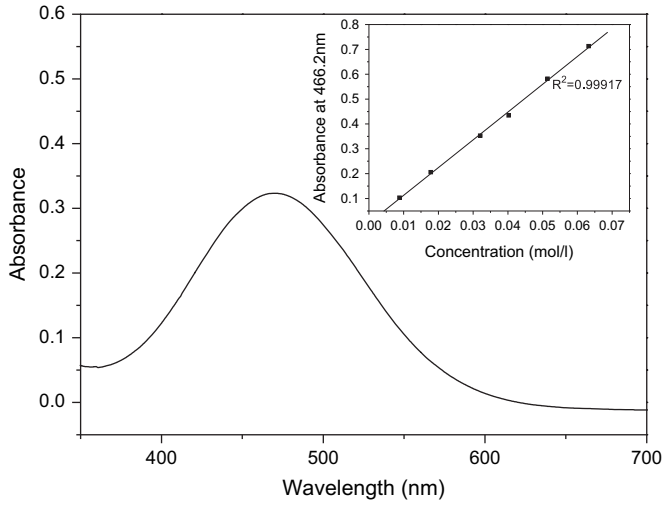

Fig. 3. UV spectrum of the PCL (Table 1, **H2**) obtained by the anionic polymerization of CL by aluminum tri(4-oxy-TEMPO) (solvent: toluene).

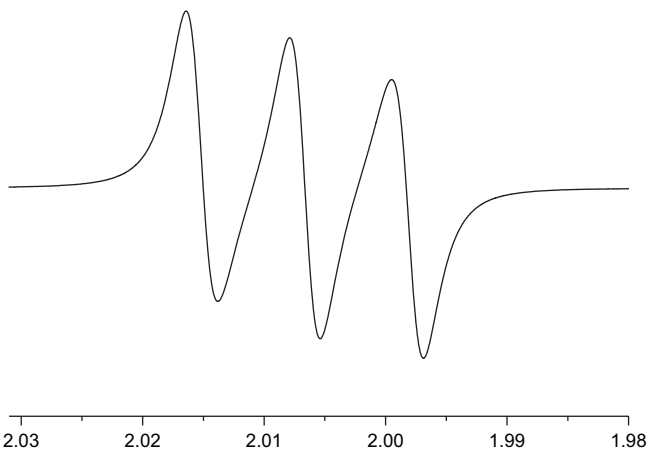

Fig. 4. ESR spectrum of the PCL (Table 1, **H2**; solvent: benzene, at room temperature).

Table 2
Radical polymerization of 4-vinylpyridine by BPO using TEMPO-terminated PCL

Copolymers	Initiator[a]	M_n (NMR)[b]	M_n (GPC)[c]	M_w/M_n[d]	M (P4VP)/n(PCL)[e]
B1	**H1**	24 900	26 000	1.30	8.8
B2	**H2**	23 300	20 500	1.26	3.1
B3	**H2**	13 800	16 600	1.25	1.4
B4	**H2**	11 300	13 380	1.23	0.95
B5	**H3**	13 500	14 900	1.34	0.33
B6	**H4**	25 000	30 100	1.30	0.1

[a] Initiators **H1**–**H4** were from Table 1.
[b] Estimated by ^{1}H NMR based on the relative intensity of the methylene (4.1 ppm) in the PCL and the protons of pyridine ring (8.3 ppm) in the P4VP.
[c] Determined by GPC using PS standards.
[d] Polydispersity index: determined by GPC.
[e] m/n = molar ratio of P4VP and PCL in the block copolymer.

ring at 1609 cm^{-1} provides the evidence that the block copolymer is indeed formed. Moreover, the GPC profile corresponding to P4VP-*b*-PCL (Fig. 1b) shows a peak shifting to a higher molecular weight compared to that of the PCL macroinitiator (Fig. 1a) while no shoulder peak can be observed. The polydispersities of the diblock copolymers remain relatively low, less than 1.30. All of the resulted block copolymers show a sharp and unimodal distribution GPC curves. Based on analyses mentioned above, these block copolymers contain two different segments of PCL and P4VP connected by the TEMPO. These results imply that this 4-hydroxy-TEMPO can be used as the transforming agent for living anionic and cationic polymerizations into living radical. The data related to the molecular weights and polydispersities of these block copolymers are summarized in Table 2.

These copolymers exhibit two glass transitions and one melting endotherm in their DSC thermograms. The DSC thermograms of the TEMPO-terminated PCL and the block copolymer are illustrated in Fig. 6 where the copolymer has the glass transition temperatures for both the amorphous phases of PCL block (−55 °C) and the P4VP block (154 °C). The melting endotherm (53 °C) for the crystalline PCL block

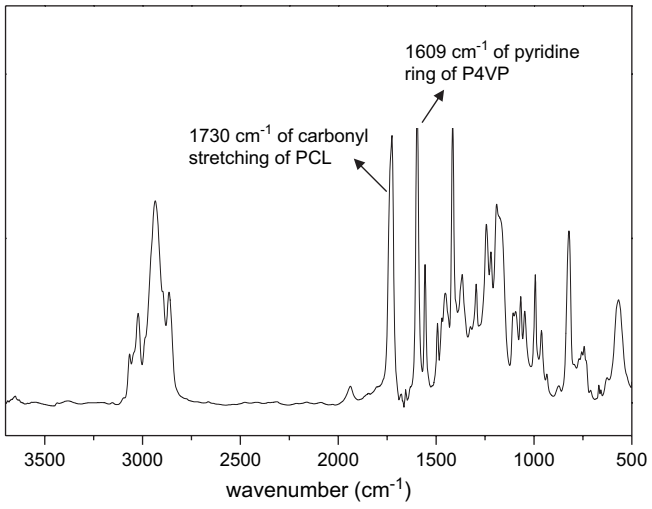

Fig. 5. FTIR spectra of the copolymer, which was obtained by the radical polymerization of styrene by BPO using PCL (Table 2, **B2**). (solvent: $CDCl_3$).

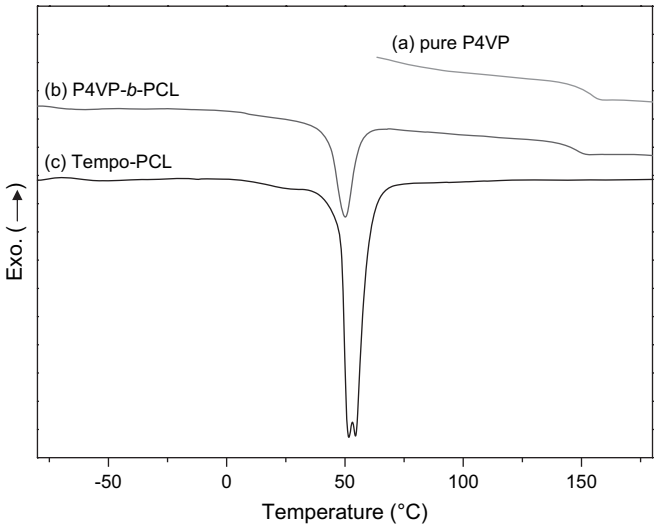

Fig. 6. DSC spectra of (a) the pure P4VP (purchased from Aldrich), (b) the copolymer (Table 2, **B2**) and (c) tempo-terminated PCL prepolymer (Table 1, **H2**).

can also be observed in the thermogram of the copolymer, as shown in Fig. 6b. The glass transitions and melting endotherm are in close agreement with those characteristics based on each of their respective homopolymers. From these results, it seems reasonable to infer that the P4VP-*b*-PCL semicrystalline diblock copolymer in bulk state is at a microphase-separated state. The segregated domains individually behave as corresponding homopolymers. Therefore, these components are expected to promote microphase segregation in bulk or in solution state.

3.3. Aggregation morphologies of P4VP-b-PCL diblock copolymer in toluene/DCM mixture

Due to the different nature between the amorphous P4VP and the crystalline PCL blocks, these copolymers are expected to undergo self-assembly into nanosized micelles with various shapes and dimensions induced by the selective solvent systems. It is well-known that changing selective solvent can shift the microphase separation of block copolymers, stabilizing the disordered state or resulting in self-assembled structures from spherical micelles to cylinders, vesicles, and lamellae [47]. As a general procedure, the block copolymer under study was firstly dissolved in a good solvent for both blocks with a typical concentration of 1 mg/mL. A second non-solvent, a poor solvent for one of the blocks, was then added to the polymer solution very slowly. We chose different solvent systems to study the effect.

In the toluene/dichloromethane (toluene/DCM) solvent system, diblock copolymers of P4VP-*b*-PCL with block ratios m/n ranging from 0.1 to 8.8 were firstly dissolved in the common solvent of DCM and then the non-solvent toluene was added slowly to induce phase separation and aggregation of the P4VP block. Eventually, the P4VP block condensed gradually and the PCL block constituted the outer shell of the particles. In this system, the influences of the block copolymer

composition and the volume ratio of the binary solvent mixture were subsequently investigated. The TEM micrographs of aggregates of copolymers **B1**–**B6** formed in toluene/DCM (9/1 v/v%) system with identical initial concentration of 1 mg/mL are shown in Fig. 7 (Table 3). Spherical micelles were formed by the diblock copolymer **B6** (block ratio $m/n = 0.1$), which has the longest PCL block and the lowest P4VP content (Fig. 7a). These spheres are nearly identical in sizes about ~20 nm. Secondary aggregation tends to occur to form sphere necklace due to interaction between micelles (Fig. 7b, copolymer **B5**). When P4VP contents are higher ($m/n > 0.95$), these block copolymers favor the formation of bilayer structures, including multilamellar vesicles, bowl-shaped vesicles, porous spheres, and large compound micelles consisting of inverse micelles.

Depending on the organic solvent employed, aggregates from spheres to rods, to vesicles, and eventually to compound micelles have been reported by Eisenberg and Zhang [20]. The core chain stretching, corona repulsion and interfacial tension between the solvent and the micellar core are believed to be main parameters dominating multi-morphological aggregate formation [20]. When the length of PCL is very long, the repulsive interactions among intercoronal chains exceed the interfacial energies and dominate the equilibrium structure. The block copolymer hence favors the formation of star-like spherical micelles with extended PCL corona. As the length of the PCL is decreased, the corona repulsion becomes relatively weak and more chains can enter the aggregates. As a result, the bilayer structures with a smaller surface area per PCL coil chain and low total interfacial energies are favored, rather than spherical micelles. As shown in Fig. 7c, vesicles are formed by the copolymer **B4** ($m/n = 0.95$) which is composed of nearly equal length of each block. As the m/n ratio is further increased to 1.4, bowl-shaped structures are obtained (Fig. 7d), the wall thickness of the bottom is significantly greater than that of the edges.

Table 3
Summary of the structural parameters of micelles formed by copolymer **B1**–**B6** under different conditions

Copolymers	Solvent system	
	Toluene/DCM	Methanol/DCM
B1	LCMs	Spheres
B2	Porous spheres	Rod-like (worm-like)
B3	Bilayer vesicles (bowl-shaped)	Vesicle
B4	Multilayer vesicles	Deformed vesicles
B5	Pearl necklace	Unclosed bilayers with lamella
B6	Spheres	Lamella

Bowl-shaped morphology was first observed by Riegel and Eisenberg in PAI–PS–PAI triblock copolymers [48]. The authors reported that the formation of the bowl-shaped structure involves a mechanism similar to that of porous spheres and large compound micelles (LCMs). All the three kinds of aggregates mentioned above consist of assemblies of inverse micelles in which the short hydrophilic blocks form the cores and the hydrophobic blocks form the continuous matrix. In this case, bowl-shaped aggregates are obtained in the copolymer **B3** in which the PCL block is relatively short ($m/n = 1.4$, Fig. 7d). When toluene is gradually added to the solution of the copolymer **B3**, the solvent becomes progressively less favorable for the P4VP segments. The polymer chains lose their

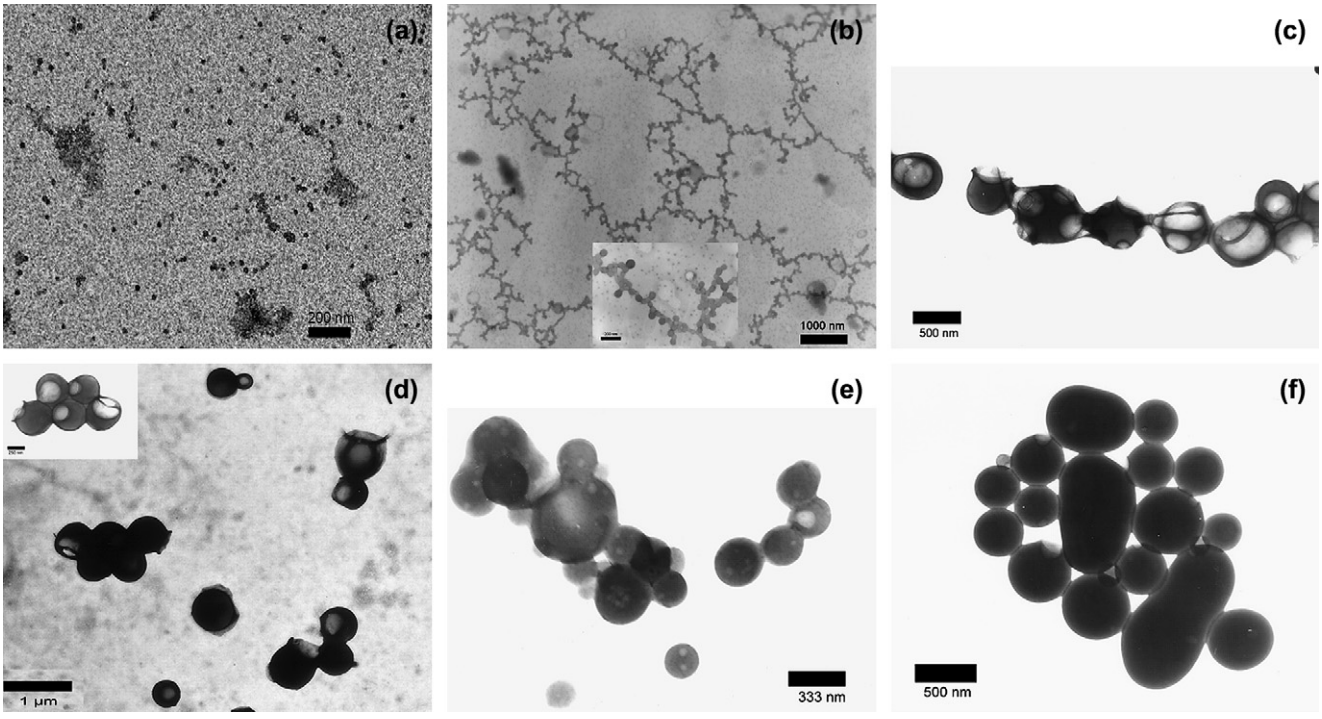

Fig. 7. TEM images of various morphologies obtained from the diblock copolymer in toluene/DCM (9/1 v/v%): (a) sphere made from **B6**, (b) sphere necklace made from **B5**, (c) multilayer vesicles made from **B4**, (d) bowl-shaped vesicles made from **B3**, (e) porous spheres made from **B2**, and (f) LCM made from **B1**.

solubility at higher toluene content and associate themselves to form spherical aggregates. Parts of these PCL segments are buried inside the aggregates and some PCL units probably segregate to the interface between the aggregates or the external solution and serve to stabilize the aggregates. When the length of PCL is further decreased, the solubility of the diblock copolymers is further reduced under the same solvent composition. Porous spheres and eventually LCM structures are formed in the copolymers **B2** and **B1** and their respective TEM images are shown in Fig. 7e and f.

On the other hand, it is known that with different compositions of solvent/non-solvent mixtures, block copolymer aggregation can be in the forms of micelles, cylinders, or vesicles of PS-*b*-PAA in DMF/water system [49]. We found that morphologies of the P4VP-*b*-PCL diblock copolymer can also be tuned by changing compositions of toluene and DCM in the binary solvent mixture. Fig. 8 shows resulting micelles self-assembled by the copolymer **B2** with the block ratio $m/n = 3.1$ at various toluene contents ranged from 10 to 90 vol%. The results reveal that when the binary solvent mixture with toluene content is below 20 vol%, spheres are formed, as shown in Fig. 8a. As the content of toluene is increased up to 50%, vesicles with various sizes are formed while monodispersed vesicles are formed with the content of toluene of about 30–40 vol% (Fig. 8c and d). Eventually, porous spheres are developed at a relatively high content of toluene (90 vol%, Fig. 7e). These structural changes by varying solvent compositions are very similar to the results reported by Shen et al. in PS-*b*-PAA at different water contents [57]. They depict a diagram of the free energies of formation of various morphologies from single chains as a function of the water content to illustrate the thermodynamical stability of each state of morphological changes [49]. In our work, rods do not appear with the change of solvent compositions, probably due to the fast thermodynamic transitions. However, we do observe a transition state between spheres to vesicles. As we tune the content of toluene to 25 vol%, a coexisting structure consisting of spheres, bilayer lamella and vesicles is formed. It is known that the vesicles can easily form when the bilayer bending elasticity is low and the surface tension is high. As shown in Fig. 8b, some vesicles are formed among these bilayer structures which may be a precursor of the monodispersed vesicles [50].

3.4. Aggregation morphologies of P4VP-b-PCL diblock copolymer in methanol/DCM mixture

When the selective solvent changes from toluene to methanol, a non-solvent for PCL blocks, the P4VP blocks become the outer part of the aggregates. Fig. 9 shows various morphologies formed by P4VP-*b*-PCL copolymers with the same initial concentration of 1 mg/mL but different block ratios. Fig. 9a shows monodispersed spherical aggregates from **B1**. Aggregates with short interconnected rods morphology are obtained when the block ratio is decreased to 3.1 (**B2**, Fig. 9b), most of these aggregates have relatively uniform diameter but differ widely in rod cylinder lengths. Hemispherical caps are clearly seen at the cylinder ends and some spheres are still present. As the *m*/*n* ratio is further reduced, polydispersed and

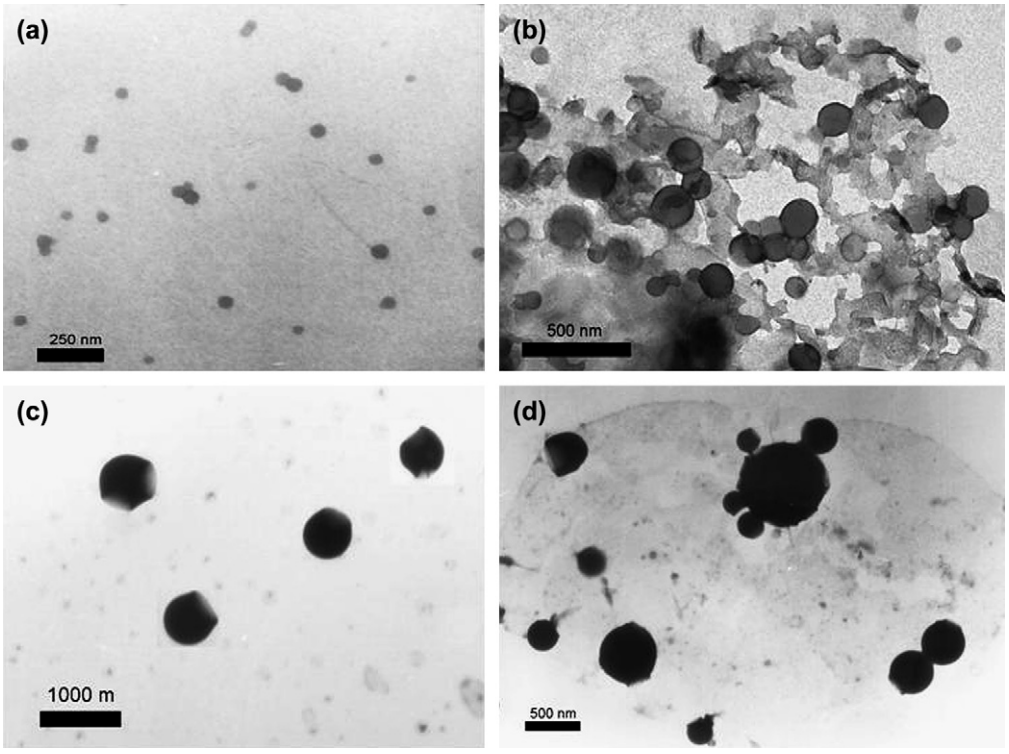

Fig. 8. TEM images of morphological changes of **B2** on addition of toluene in toluene/DCM binary solvent mixture for initial concentration at 1.00 mg/mL: (a) spheres at 20 v/v% toluene, (b) coexisting structure consists of spheres, bilayer lamella and vesicles upon addition of toluene to 25 v/v%, (c) monodispersed vesicles at 30 v/v% toluene, and (d) vesicles with various sizes at 50 v/v% toluene.

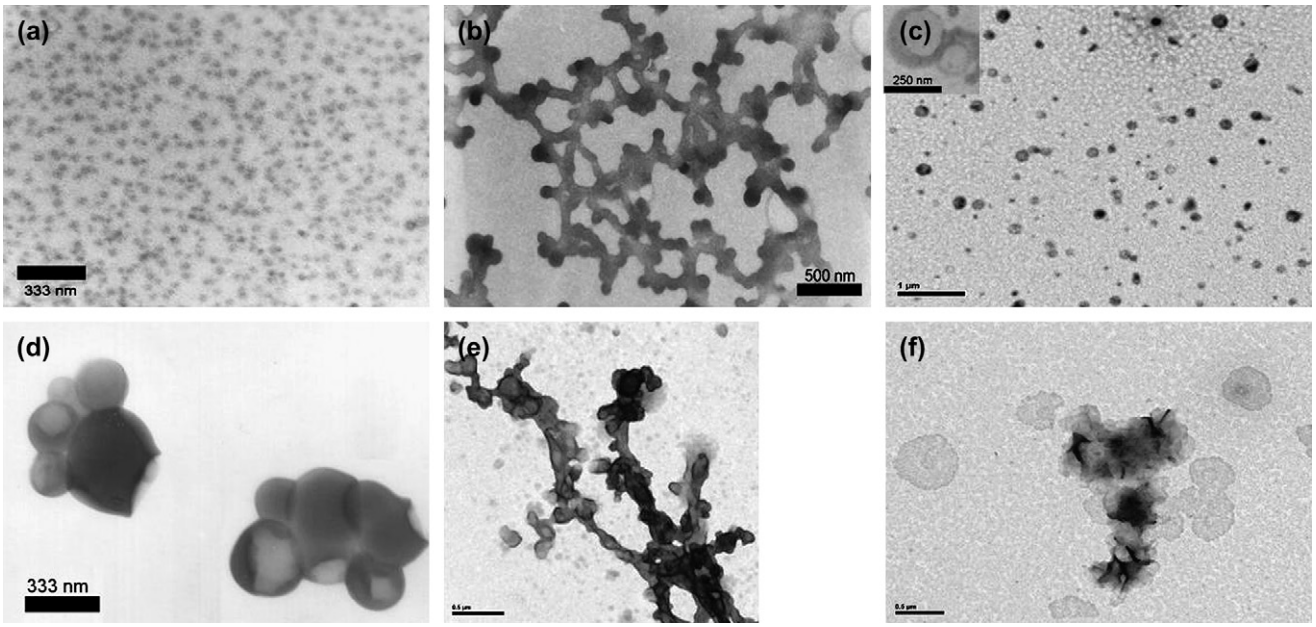

Fig. 9. TEM images of various morphologies obtained from the diblock copolymer in methanol/DCM (9/1 v/v%): (a) sphere made from **B1**, (b) worm-like rods made from **B2**, (c) vesicles made from **B3**, (d) deformed vesicles made from **B4**, (e) unclosed bilayers with lamella made from **B5**, and (f) platelet lamella made from **B6**.

deformed vesicles are formed for block copolymers **B3** and **B4** as shown in Fig. 9c and d. In copolymer **B5**, the aggregate morphology transforms into a coexisted structure composed of vesicles, lamella and unclosed bilayers. When the *m*/*n* ratio is equal to 0.11 (the lowest P4VP block content in **B6**), aggregates consisting of lamella are obtained as shown in Fig. 9f.

As mentioned, P4VP-*b*-PCL is a semicrystalline diblock copolymer, the interplay between crystallization and the dissolution effect, as well as the segregation between unlike blocks, provides a critical factor in dictating the final aggregated morphologies. In an attempt to gain some insight into the nature of the micellar core of P4VP-*b*-PCL, WAXS experiments were undertaken. Films of aggregates formed by the block copolymers **B1**–**B6** were deposited on an aluminum substrate from methanol/DCM (95/5 v/v%) and the WAXS patterns were obtained. Fig. 10a illustrates the diffraction pattern of the platelet structural aggregates from the copolymer **B6**, in which strong crystalline diffraction peaks at 21.3° and 23.6° from the PCL parts are observed. The crystallization and melting behaviors of PCL have been extensively studied, and it has been established that crystallization of PCL occurs by the spontaneous formation of folded chain structures within a lamellar lattice [51]. In contrast with amorphous diblock copolymers in a selective solvent that form spherical micellar structures, semicrystalline diblock copolymers self-assemble in solution to form large platelets consisting of a thin chain-folded lamellar domain within layers of the solvated amorphous block. The pattern of the micellar cores as shown in Fig. 10a closely matches to that of the pure PCL, implying that these core blocks undergo chain-fold crystallization within the micelles [52]. Therefore, these plate-like lamellae formed from copolymer **B6** possessing the largest molar ratio of PCL block is believed to be driven by crystallization of the PCL core domains [53]. Similar XRD patterns are also observed in other aggregates formed by the copolymers **B2**–**B5** while no signal is observed in the copolymer **B1** (Fig. 10b). The results indicate that copolymer **B1** (the lowest molar ratio) in solution performs as an amorphous polymer to form spherical micelles that are only affected by the packing parameters. On the other hand, since most of the aggregates formed by these copolymers exhibit crystalline nature, it is suggested that the detailed morphology of such aggregates is determined by the balance of entropic forces resulting from the stretching of the P4VP coils and the enthalpic contribution from the PCL chain folding [54]. In the formed vesicle and lamella structures, the membrane consists entirely of the chain-folded PCL lamella with PEO corona facing the external solution. Obviously, the

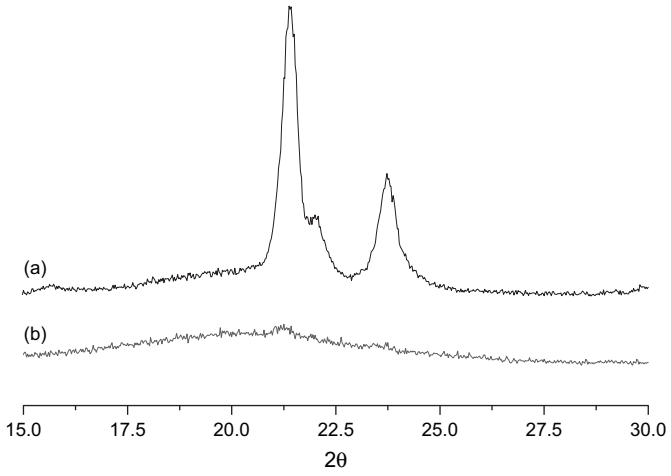

Fig. 10. XRD patterns of aggregates formed by (a) copolymer **B6**, which possess a platelet lamella structures and (b) copolymer **B1** with spherical micelles.

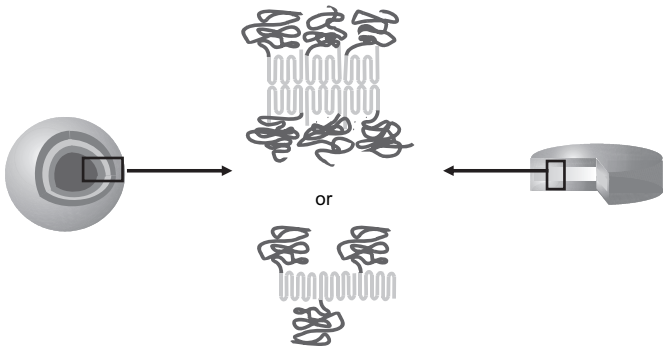

Fig. 11. Schematic representation of bilayer or monolayer packing of coil–crystalline lamella in polymeric micelles.

crystalline PCL affects more the resultant structure of aggregates at high PCL composition block copolymers such as **B5** and **B6**. The aggregate morphologies consist of chain-folded PCL lamella as illustrated in Fig. 11.

4. Conclusions

A series of well-defined diblock copolymers of P4VP-*b*-PCL have been obtained via a new synthetic procedure by anionic ring-opening polymerization of ε-caprolactone followed by living nitroxide-mediated free radical polymerization (NMP) of 4-vinylpyridine with a bifunctional initiator. Due to the different nature between the PCL and P4VP blocks, these copolymers can undergo self-assembly into nanosized micelles induced by selective solvent systems. These copolymers with different block compositions and molecular weights are able to self-assemble into different forms of aggregates in toluene/DCM or methanol/DCM. In toluene/DCM system, the relative block length plays an important role in affecting the resulted supramolecular architecture. By gradually increasing the toluene content, the **B2** block copolymer forms spheres first, then shifts to a mixture of vesicles and bilayer structures, vesicles, and finally transforms into porous spheres at high toluene content. In methanol/DCM system, the structure of aggregates is determined by the balance of entropic forces resulting from the stretching of the P4VP coils and the enthalpic contribution from the PCL chain folding since the crystalline PCL forms the core in the micelle. The crystalline of PCL in the cores of aggregates was further confirmed by XRD, indicating that the PCL exists as chain-folded lamella structure in the micelle.

References

[1] Hamley IU. The physics of block copolymers. Oxford, UK: Oxford University Press; 1998.
[2] Foerster S, Antonietti M. Adv Mater 1998;10:195.
[3] Hadjichristidis N, Pispas S, Floudas GA. Block copolymers synthetic strategies, physical properties, and applications. Hoboken: John Wiley & Sons; 2003.
[4] Cgatterjii U, Jwearjka SK, Mandal BM. Polymer 2005;46:10699.
[5] Cao L, Manners I, Winnik MA. Macromolecules 2002;35:8258.
[6] Bhargava P, Zheng JX, Li P, Quirk R, Harris FW, Cheng SZD. Macromolecules 2006;39:4880.
[7] Ding J, Liu G, Yang M. Polymer 1997;38:5497.
[8] Ding JF, Liu GJ. J Phys Chem B 1998;102:6107.
[9] Zhou SQ, Chu B. Macromolecules 1998;31:7746.
[10] Zhang W, Jiang X, He Z, Xiong D, Zheng P, An Y, et al. Polymer 2006;47:8203.
[11] Jain S, Bates FS. Science 2003;300:460.
[12] Raez J, Manners I, Winnik MA. J Am Chem Soc 2002;124:10381.
[13] Jain S, Bates FS. Macromolecules 2004;37:1511.
[14] Hoppenbrouwers E, Li Z, Liu G. Macromolecules 2003;36:876.
[15] Nardin C, Hirt T, Leukel J, Meier W. Langmuir 2000;16:1035.
[16] Kukula H, Schlaad H, Antonietti M, Forster S. J Am Chem Soc 2002;124:1658.
[17] Li Z, Kesselman E, Talmon Y, Hillmyer MA, Lodge TP. Science 2004;306:98.
[18] Jenekhe SA, Chen XL. Science 1998;279:1903.
[19] Zhang L, Eisenberg A. Science 1995;268:1728.
[20] Zhang L, Eisenberg A. J Am Chem Soc 1996;118:3168.
[21] Zhang L, Yu K, Eisenberg A. Science 1996;272:1777.
[22] Discher BM, Won YY, Ege D, Lee JCM, Bates FS, Discher DE, et al. Science 1999;284:1143.
[23] Bermudez H, Brannan AK, Hammer DA, Bates FS, Discher DE. Macromolecules 2002;35:8203.
[24] Hartgerink JD, Beniash E, Stupp SI. Science 2001;294:1684.
[25] Ludwigs S, Boker A, Voronov A, Rehse N, Magerle R, Krausch G. Nature 2003;2:744.
[26] Loos K, Boker A, Zettl H, Zhang M, Krausch G, Muller AHE. Macromolecules 2005;38:873.
[27] Zhao C, Winnik MA, Riess GC, Croucher MD. Macromolecules 1990;6:514.
[28] Massey J, Power KN, Manners I, Winnik MA. J Am Chem Soc 1998;120:9533.
[29] Kataoka K, Harada A, Nagasaki Y. Adv Drug Delivery Rev 2001;47:113.
[30] Savic R, Luo LB, Eisenberg A. Science 2003;300:615.
[31] Rosler A, Vandermeulen GWM, Klok HA. Adv Drug Delivery Rev 2001;53:95.
[32] Cameron NS, Corbierre MK, Eisenberg A. Can J Chem 1999;77:1311.
[33] Yu K, Eisenberg A. Macromolecules 1998;31:3509.
[34] Zhang LF, Shen HW, Eisenberg A. Macromolecules 1997;30:1001.
[35] Ouhasi T, Stevens C, Teyssie P. Makromol Chem Suppl 1975;1:191.
[36] Yoshida E, Sugita A. Macromolecules 1996;29:6422.
[37] Matyjaszewski K, Shigemoto T, Frechet JMJ, Leduc M. Macromolecules 1996;29:4167.
[38] Hawker CJ. J Am Chem Soc 1994;116:11185.
[39] Hawker CJ, Bosman AW, Harth E. Chem Rev 2001;101:3661.
[40] Fischer H. Chem Rev 2001;101:3581.
[41] Solomon DH, Rizzardo E, Cacioli P. U.S. Patent 4,581,429; 1986.
[42] Georges MK, Veregin RPN, Kazmaier PM, Hamer GK. Macromolecules 1993;26:2987.
[43] Jia X, Mingqian L, Han S, Wang C, Wei Y. Mater Lett 1997;31:137.
[44] Bohrisch J, Wendler U, Jaeger W. Macromol Rapid Commun 1997;18:975.
[45] Jacobs C, Dubois P, Jerome R, Teyssie P. Macromolecules 1991;24:3027.
[46] Kroschwitz JI, editor. Vinylpyridine polymers. Encyclopedia of polymer science and engineering. 2nd ed., vol. 17. New York: J. Wiley & Sons; 1989. p. 569.
[47] Shen H, Eisenberg A. Macromolecules 2000;33:2561.
[48] Riegel IC, Eisenberg A. Langmuir 2002;18:3358.
[49] Shen H, Eisenberg A. J Phys Chem B 1999;103:9473.
[50] Antonietti M, Foerster S. Adv Mater 2003;15:1323.
[51] Gan ZH, Jiang BZ, Zhang J. J Appl Polym Sci 1996;59:961.
[52] Lin EK, Gast AP. Macromolecules 1996;29:4432.
[53] Vilgis T, Halperin A. Macromolecules 1991;24:2090.
[54] Richter D, Schneiders D, Monkenbusch M, Willner L, Fetters LJ, Huang JS, et al. Macromolecules 1997;30:1053.